Copper(II) and Copper(I) Complexes with an Open-Chain N_4 Schiff Base Ligand Modeling CuZn Superoxide Dismutase: Structural and Spectroscopic Characterization and Kinetics of Electron Transfer

Jürgen Lange, Horst Elias,* and Helmut Paulus[†]

Institut für Anorganische Chemie, Technische Universität Darmstadt, Petersenstrasse 18, D-64287 Darmstadt, Federal Republic of Germany

Jörg Müller and Ulrich Weser

Anorganische Biochemie, Physiologisch-Chemisches Institut der Eberhard-Karls-Universität Tübingen, D-72076 Tübingen, Federal Republic of Germany

Received January 31, 2000

The structure of the complex $[Cu^{II}(PuPy)](ClO_4)_2$ (PuPy = L = 1,8-bis(2-pyridyl)-2,7-diazaoctadiene-1,7) and the structure of the corresponding copper(I) complex were determined. In $Cu^{II}L(ClO_4)_2$, a model compound with CuZnSOD activity, the unit $Cu^{II}L^{2+}$ has a tetrahedrally distorted square-planar N_4 coordination geometry. The copper(I) complex with L was found to be dimeric, $(Cu^{I}L)_2(ClO_4)_2$·DMF (DMF = *N*,*N*-dimethylformamide). The binuclear unit $(Cu^{I}L)_2^{2+}$ has a helical structure with two ligands L bridging the two copper atoms to provide tetrahedral N_4 coordination of each copper(I). In solutions of $(Cu^{I}L)_2(ClO_4)_2$·DMF, solvent-dependent dissociation occurs according to D ⇌ 2M (D = $(Cu^{I}L)_2^{2+}$; M = $Cu^{I}LS_x^{+}$; S = solvent). Stopped-flow spectrophotometry was used to determine the rate constants for the dissociation of the dimer D (k_M) and dimerization of the monomer M (k_D) for S = acetonitrile and DMF. Equilibrium constants $K_{dim} = k_M/k_D$ were determined spectrophotometrically. In aqueous solution, the oxidation of the dimer $(Cu^{I}L)_2^{2+}$ by $Co^{III}(NH_3)_5Cl^{2+}$ and *cis*- and *trans*-$Co^{III}(en)_2Cl_2^{+}$ follows a second-order rate law, rate = $k_{ox}[(Cu^{I}L)_2^{2+}][Co(III)]$. Data for rate constant k_{ox} and for the activation parameters $\Delta H^{\ddagger}$ and $\Delta S^{\ddagger}$ are presented. In DMF, the oxidation of $(Cu^{I}L)_2^{2+}$ by $Co^{III}(NH_3)_5Cl^{2+}$ occurs via the monomer $Cu^{I}L(DMF)_x^{+}$ and the dissociation of $(Cu^{I}L)_2^{2+}$ becomes rate-controlling. The reduction of $Cu^{II}L^{2+}$ by $Ru^{II}(edta)H_2O^{2-}$ was found to be too fast to be resolved by stopped-flow spectrophotometry. The kinetic results are discussed mechanistically in terms of the redox switch aspects of the system.

Introduction

Superoxide dismutases (SODs) catalyze the proton-dependent dismutation of two superoxide radical anions to molecular oxygen and hydrogen peroxide. The biological functions of SODs are very important because they prevent oxidative damage and inflammation, due to subsequent formation of oxygen intermediates derived from the superoxide, and are involved in anticancer and antiaging mechanisms.[1−3] Copper zinc superoxide dismutase, CuZnSOD, is a dimeric protein with two identical subunits bonded noncovalently.[1] Each subunit contains one copper(II) and one zinc(II) ion in the oxidized state of the metalloenzyme. The Cu^{2+} ion is N_4-coordinated in a square-planar geometry with tetrahedral distortion. During catalysis, copper is the redox partner of the superoxide radical.

The biological importance of CuZnSOD has led to various attempts to mimic the redox function of the copper site with synthetic copper complexes.[4] Weser and co-workers designed the di-Schiff-base ligand PuPy = 1,8-bis(2-pyridyl)-2,7-diazaoctadiene-1,7, resulting from the condensation reaction of two molecules of pyridine-2-carbaldehyde with one molecule of 1,4-diaminobutane. The butylene bridge in this open-chain N_4 ligand was thought to be long and flexible enough to allow (distorted) square-planar coordination for Cu(II) and (distorted) tetrahedral coordination for Cu(I). The corresponding copper(II) complex $Cu^{II}(PuPy)^{2+}$ (see Chart 1) was indeed found to possess SOD activity (3% of native SOD)[5a,b] and also anticancerogenic[5c] and antirheumatic activity.[5d] The cation $Cu^{II}(PuPy)^{2+}$ tends to become five-coordinate, and the coordination geometry of the cations $Cu^{II}(PuPy)TU^{2+}$,[6] $Cu^{II}(PuPy)I^{+}$,[7] and $Cu^{II}(PuPy)Br^{+}$,[8] as determined by X-ray crystallography, is that of a distorted square pyramid. To our knowledge, there is no report so far on the X-ray structure analysis of the cations $Cu^{II}(PuPy)^{2+}$ and $Cu^{I}(PuPy)^{+}$ by X-ray crystallography.

* To whom correspondence should be addressed. E-mail: Elias@tu-darmstadt.de.

[†] Present address: Technische Universität Darmstadt, Fachbereich Materialwissenschaft, Fachgebiet, Strukturforschung.

(1) Bannister, J. V.; Bannister, W. H.; Rotilio, G. *CRC Crit. Rev. Biochem.* **1987**, *22*, 111.
(2) Holm, R. H.; Kennepohl, P.; Solomon, E. I. *Chem. Rev.* **1996**, *96*, 2239.
(3) Miller, A.-F.; Sorkin, D. L. *Comments Mol. Cell. Biophys.* **1997**, *9*, 1.
(4) Gaertner, A.; Weser, U. *Top. Curr. Chem.* **1986**, *132*, 1.
(5) (a) Linss, M.; Weser, U. *Inorg. Chim. Acta* **1986**, *125*, 117. (b) Linss, M.; Weser, U. *Inorg. Chim. Acta* **1987**, *138*, 163. (c) Miesel, R.; Weser, U. *Free Radical Res. Commun.* **1990**, *11*, 39. (d) Miesel, R.; Weser, U. Ger. Offen. DE 3,912,642 (Cl. C07D401/12), 1990.
(6) Ferrari, M. B.; Corradi, A. B.; Fava, G. G.; Grasselli Palmieri, C.; Nardelli, M.; Pelizzi, C. *Acta Crystallogr., Sect. B* **1973**, *29*, 1808.
(7) Carradi, A. B.; Nardelli, M.; Pelizzi, C. *Koord. Khim.* **1975**, *1*, 1134.
(8) Pajunen, A.; Pajunen, S. *Acta Crystallogr.* **1986**, *C42*, 53.

10.1021/ic000097q CCC: $19.00 © 2000 American Chemical Society
Published on Web 07/01/2000

Chart 1

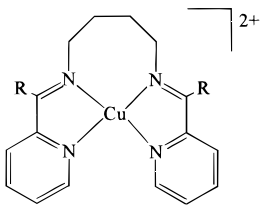

$R = H: Cu^{II}(PuPy)^{2+} = Cu^{II}L^{2+}$

$R = methyl: Cu^{II}(PuMePy)^{2+}$

$R = phenyl: Cu^{II}(PuPhPy)^{2+}$

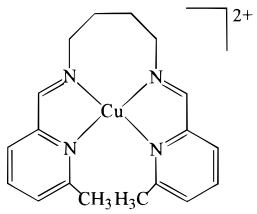

$Cu^{II}(Pu\text{-}6\text{-}MePy)^{2+}$

The introduction of substituents R = methyl[9] and R = phenyl[10] at the imine carbon atoms of the ligand (see Chart 1) was found to increase the stability of the corresponding copper(II) complexes $Cu^{II}(PuMePy)^{2+}$ and $Cu^{II}(PuPhPy)^{2+}$ as well as the SOD activity. In particular, the phenyl-substituted complex $Cu^{II}(PuPhPy)^{2+}$ is a remarkably effective CuZnSOD mimic and survives competitive biochelation.[10]

The work carried out by Linss and Weser[5a,b] on the SOD activity of the cation $Cu^{II}(PuPy)^{2+}$ implies that the reduction according to

$$Cu^{II}(PuPy)^{2+} + e^- \rightarrow Cu^{I}(PuPy)^{+} \qquad (1)$$

leads to the monomeric copper(I) species $Cu^{I}(PuPy)^{+}$, which was not isolated. We used the salt $Cu^{I}(CH_3CN)_4ClO_4$ to prepare the copper(I) complex, and in *N*,*N*-dimethylformamide (DMF) we obtained a product of composition $Cu^{I}(PuPy)ClO_4 \cdot 0.5$ DMF. To our surprise, the UV/vis spectra of this compound were concentration-dependent. This finding and the fact that, compared to CuZnSOD, $Cu^{II}(PuPy)^{2+}$ reacts with superoxide by 3 orders of magnitude more slowly[10] led us to study the properties of the copper(I) complex in greater detail and also to investigate the kinetics of electron-transfer according to

$$Cu^{I}(PuPy)^{+} + Ox \rightarrow Cu^{II}(PuPy)^{2+} + Red \qquad (2)$$

$$Cu^{II}(PuPy)^{2+} + Red \rightarrow Cu^{I}(PuPy)^{+} + Ox \qquad (3)$$

with one-electron oxidants Ox and reductants Red.

Experimental Section

Chemicals and Reagents. $Cu(ClO_4)_2 \cdot 6H_2O$, 1,4-diaminobutane, pyridine-2-carbaldehyde, *N*,*N*-dimethylformamide (DMF), and acetonitrile were of reagent grade quality and were used without further purification. Deionized water was doubly distilled in a quartz apparatus before use.

$[Cu^{I}(CH_3CN)_4]ClO_4$,[11] $[Co^{III}(NH_3)_5Cl](ClO_4)_2$,[12] *cis*- and *trans*-$[Co^{III}(en)_2Cl_2]Cl$,[13] $[Cu^{II}(PuPy)](ClO_4)_2$,[5a] $[Cu^{II}(PuMePy)](NO_3)_2$,[9] $[Cu^{II}(PuPhPy)](NO_3)_2 \cdot 0.5H_2O$,[14]and the cation $[Ru^{II}(edta)H_2O]^{2-}$[16] were prepared as described. Crystals of $[Cu^{II}(PuPy)](ClO_4)_2$ suitable for X-ray diffraction work were obtained by slow evaporation of a saturated solution of the complex in ethanol. (*WARNING!* Perchlorate salts are potentially explosive. They should be handled with caution and in small quantities only.)

Table 1. Equilibrium Constants K_{py} for the Addition of Pyridine to the Copper(II) Complexes According to Reaction 4 at 298 K in Aqueous Solution

complex	K_{py}, M^{-1}
$Cu(PuPy)^{2+}$	18.5 ± 1.0
$Cu(PuMePy)^{2+}$	9.0 ± 0.5
$Cu(PuPhPy)^{2+}$	14.0 ± 0.5

Ligand 1,8-Bis(2-pyridyl)-2,7-diazaoctadiene-1,7 (PuPy). A solution of 4.28 g of pyridine-2-carbaldehyde (40 mmol) in 50 mL of ethanol was stirred at 298 K, and 1.76 g of 1,4-diaminobutane (20 mmol) was added dropwise. After partial removal of the solvent, recrystallization from ethanol yielded 2.8 g (53%) of pale-yellow crystals. Anal. Calcd for $C_{16}H_{18}N_4$: C, 72.18; H, 6.77; N, 21.05. Found: C, 72.12; H, 6.90; N, 20.98.

$[Cu^{I}(PuPy)]_2(ClO_4)_2 \cdot$DMF. In an argon box, 6.36 g of $[Cu^{I}(CH_3CN)_4]ClO_4$ (20 mmol) were dissolved in 200 mL of CH_3CN. In small portions, 5.32 g of the ligand PuPy (20 mmol) were added to the stirred solution, which became red-brown. After the solution was stirred for 3 h, the solvent was removed and the resulting brown powder was recrystallized in a small volume of DMF. After standing for a few days, red-brown crystals had separated (4.2 g, 45% yield), which were suitable for X-ray diffraction work. ^{1}H NMR (ppm, DMF-d_7, 296 K): δ 7.5−8.5 (m, 8 H + 2 H), 3.90 (m, br, 4 H), 1.75 (m, 4 H). IR (cm^{-1}, KBr): 3078 (m), 2925 (m), 2867 (m), 1662 (s), 1600 (m), 1080 (vs). UV/vis (nm, M^{-1} cm^{-1}, H_2O): 478 (13600 ± 400). Anal. Calcd for $C_{35}H_{43}Cl_2Cu_2N_9O_9$ (931.76): C, 45.11; H, 4.62; N, 13.53. Found: C, 44.94; H, 4.54; N, 13.66.

In Situ Preparation of the Copper(I) Complexes with the Ligands PuMePy and PuPhPy. For UV/vis spectrophotometric characterization, aqueous solutions of the copper(I) complexes with PuMePy and PuPhPy were prepared by in situ reduction of the corresponding copper(II) complexes with amalgamated zinc pellets.

Solutions. The solutions applied for the spectrophotometric and kinetic investigation of the dimer/monomer equilibrium and for the study of electron transfer were deaerated by saturation with argon.

Instrumentation. The following instruments were used: UV/vis spectra, diode array spectrophotometer (Zeiss Specord S10); NMR spectra, FT-NMR spectrometer (Bruker WM 200); IR spectra, FT-IR spectrometer (Nicolet, Impact 400); spectrophotometric monitoring of reactions with $t_{1/2} < 2$ min, multiwavelength stopped-flow spectrophotometer.[17]

Spectrophotometric Titration. Equilibrium constant K_{py} for the coordination of pyridine by the cation $Cu^{II}(PuPy)^{2+}$,

$$Cu(PuPy)^{2+} + py \overset{K_{py}}{\rightleftharpoons} Cu(PuPy)py^{2+} \qquad (4)$$

(and also by the cations $Cu^{II}(PuMePy)^{2+}$ and $Cu^{II}(PuPhPy)^{2+}$) was determined by spectrophotometric titration with pyridine in the wavelength range 400−1000 nm at pH 6 (pyridine/pyridinium buffer) in aqueous solution at $I = 0.52$ M ($NaNO_3$) and 298 K. The concentration of the complex was 2×10^{-3} M, and the concentration of pyridine covered the range 10^{-2}−2.5 M. Least-squares fitting of

$$A = \frac{A_0 + A_\infty K_{py}[py]}{1 + K_{py}[py]} \qquad (5)$$

to the {absorbance,[py]} data led to the data for K_{py} compiled in Table 1 (A_0 and A_∞ refer to the absorbance of the species $Cu^{II}(PuPy)^{2+}$ and $Cu^{II}(PuPy)py^{2+}$, respectively, at the concentration of $[Cu(PuPy)^{2+}]_0$).

Dimer/Monomer Equilibrium. Equilibrium constant K_{dim} for the dissociation of the dimeric complex $[Cu^{I}(PuPy)]_2^{2+}$ (=D) in acetonitrile and in DMF to form the monomeric species $Cu^{I}(PuPy)^{+}$ (=M) according to

(9) Luo, Q.; Lu, Q.; Dai, A.; Huang, L. *J. Inorg. Biochem.* **1993**, *51*, 655.
(10) Müller, J.; Felix, K.; Maichle, C.; Lengfelder, E.; Strähle, J.; Weser, U. *Inorg. Chim. Acta* **1995**, *233*, 11.
(11) Müller, E.; Bernardinelli, G.; Reedijk, J. *Inorg. Chem.* **1996**, *35*, 1952.
(12) Parker, O. J.; Espenson, H. *J. Am. Chem. Soc.* **1969**, *91*, 1968.
(13) Bailar, J. C. *Inorg. Synth.* **1946**, *2*, 222.
(14) The synthesis was carried out analogously to the procedure described in ref 15.
(15) Addison, A. W.; Rao, T. N.; Sinn, E. *Inorg. Chem.* **1984**, *23*, 1857.
(16) Diamantis, A. A.; Dubrawski, J. V. *Inorg. Chem.* **1981**, *20*, 1142.
(17) Drexler, C.; Elias, H.; Fecher, B.; Wannowius, K. J. *Fresenius J. Anal. Chem.* **1991**, *340*, 605.

$$D \underset{k_D}{\overset{k_M}{\rightleftharpoons}} 2M \qquad K_{dim} = k_M/k_D \tag{6}$$

was determined by the dilution method based on spectrophotometric monitoring in the wavelength range 400−600 nm. The product $[D]_0 d$ was kept constant at variable initial concentration of the dimer D and variable path length d of the cell. The observed absorbance A_{obsd} led to an apparent absorptivity ϵ_{obsd} according to $\epsilon_{obsd} = A_{obsd}/([M]_0 d)$ ($[M]_0 = 2[D] + [M]$ = total copper(I) concentration). The (A_{obsd}, $[M]_0$) data obtained were computer-fitted with

$$\epsilon_{obsd} = \left(\epsilon_M - \frac{1}{2}\epsilon_D\right)\frac{K_{dim}}{4[M]_0}\left(-1 + \sqrt{1 + \frac{8[M]_0}{K_{dim}}}\right) + \frac{1}{2}\epsilon_D \tag{7}$$

to obtain K_{dim}, ϵ_D, and ϵ_M.

Kinetics of the Dimer/Monomer Equilibrium. The kinetics of the dissociation of the dimer D according to eq 6 were investigated by the c-jump technique with a stopped-flow spectrophotometer in the wavelength range 300−600 nm at 298 K and $I = 0.2$ M ($NaClO_4$). One syringe was filled with the solution of the dimer, the other with blank solvent. The c-jump associated with this sort of stopped-flow experiment ($[D]_0 \rightarrow [D]_0/2$) was sufficient to produce a small but measurable perturbation of equilibrium 6. Least-squares fitting of the (absorbance,time) data with

$$A = (A_0 - A_\infty)[\exp(-k_{obsd}t)] + A_\infty \tag{8}$$

led to the experimental rate constant k_{obsd}, which is defined by

$$k_{obsd}^2 = 8k_M k_D[M]_0 + k_M^2 \tag{9}$$

with $[M]_0 = 2[D] + [M]$ = total copper(I) concentration.[18] The linear plot of k_{obsd}^2 vs $[M]_0$ allows the calculation of k_M and k_D from the slope ($8k_M k_D$) and from the intercept (k_M^2).

Kinetics of Electron Transfer. The kinetics of ET according to eq 2 with Ox = $[Co^{III}(NH_3)_5Cl]^{2+}$, *cis*-$[Co^{III}(en)_2Cl_2]^+$, and *trans*-$[Co^{III}(en)_2Cl_2]^+$ were studied under pseudo-first-order conditions ([Ox] ≫ $[Cu^I(PuPy)^+]$), partly at variable temperature, with argon-purged solutions of Ox and of the copper(I) complex. Fitting of eq 8 or

$$A = a_1[\exp(-k_{obsd,1}t)] + a_2[\exp(-k_{obsd,2}t)] + A_\infty \tag{10}$$

to the (absorbance,time) data led to the corresponding experimental rate constants (a_1 and a_2 are the amplitudes of the two exponentials). The reduction of the cation $Cu^{II}(PuPy)^{2+}$ with the anion $[Ru(edta)H_2O]^{2-}$ leads to monomeric $Cu^I(PuPy)^+$, which dimerizes and equilibrates according to eq 6. The (absorbance,time) data for this process were fitted with the equation[19]

$$A = \frac{a + b\exp(-k_{obsd}t)}{1 - c\exp(-k_{obsd}t)} \tag{11}$$

to obtain k_{obsd}, which allows the calculation of k_D according to

$$k_{obsd} = \frac{[D]_\infty^2 - [M]_o^2}{[D]_\infty} k_D \tag{12}$$

Crystallographic Studies. The measurements were carried out on a four-circle diffractometer (Stoe-Stadi-4) using graphite-monochromatized Mo Kα radiation ($\lambda = 0.710\,69$ Å) with $2\theta{:}\omega = 1{:}1$ scans. The structure was solved by direct methods with SHELXS-86 and refined by the least-squares method to the R values given in Table 2 with the program package SHELXL-93. The non-hydrogen atoms were refined anisotropically. All hydrogen atoms were located in the difference Fourier map. The hydrogen atom positions and a uniform isotopic displacement parameter were kept fixed during refinement.

A blue-green crystal (plate) of $[Cu^{II}(PuPy)](ClO_4)_2$ with the approximate dimensions 0.12 mm × 0.35 mm × 0.65 mm was grown as stated above. Cell constants were determined by the least-squares method from the 2θ angles of 48 reflections. The index ranges were $-17 \le h \le 6$, $0 \le k \le 8$, $-23 \le l \le 23$. An empirical absorption correction was applied ($T_{min}/T_{max} = 0.651/0.851$). The residual electron density was (+0.781)/(−0.567) e Å^{-3}. Crystal data and data collection parameters are listed Table 2.

A dark-brown prismatic crystal of $[Cu^I(PuPy)]_2(ClO_4)_2 \cdot DMF$ with the approximate dimensions 0.55 mm × 0.55 mm × 0.51 mm was grown as stated above. Cell constants were determined by the least-squares method from the 2θ angles of 50 reflections. The index ranges were $-12 \le h \le 1$, $-15 \le k \le 15$, $-18 \le l \le 18$. An empirical absorption correction was applied ($T_{min}/T_{max} = 0.546/0.620$). The residual electron density was (+0.626)/(−0.494) e Å^{-3}. Crystal data and data collection parameters are listed in Table 2.

Table 2. Crystallographic Data for $[Cu^{II}(PuPy)](ClO_4)_2$ and $[Cu^I(PuPy)]_2(ClO_4)_2 \cdot DMF$

	$[Cu^{II}(PuPy)](ClO_4)_2$	$[Cu^I(PuPy)]_2(ClO_4)_2 \cdot DMF$
chemical formula	$C_{16}H_{18}Cl_2CuN_4O_8$	$C_{35}H_{43}Cl_2Cu_2N_9O_9$
fw, g/mol	528.78	931.76
cryst syst	monoclinic	triclinic
space group	$P2_1/c$ (No. 14)	$P\bar{1}$ (No. 2)
a, Å	14.409(5)	10.354(2)
b, Å	7.511(3)	13.140(3)
c, Å	20.163(7)	15.668(3)
α, deg		96.52(1)
β, deg	109.62(1)	94.65(1)
γ, deg		91.91(1)
V, Å^3	2055.5(13)	2108.9(7)
Z	4	2
ρ_{calcd}, g/cm^3	1.709	1.467
temp, K	300(2)	299(2)
μ, mm^{-1}	1.376	1.196
λ (Mo Kα), Å	0.710 69	0.710 69
θ range, deg	1.50−24.99	1.56−24.98
no. reflns collected	5355	8691
no. independent reflns	3601 ($R_{int} = 0.0124$)	7415 ($R_{int} = 0.0127$)
no. params	291	513
R1[a] [$I > 2\sigma(I)$]	0.0572	0.0466
wR2[b]	0.1567	0.1320

[a] $R1 = \sum(|F_o| - |F_c|)/\sum|F_o|$. [b] $wR2 = \sum w(|F_o^2| - |F_c^2|)^2/\sum w|F_o^2|$.

Table 3. Selected Bond Lengths (Å) and Angles (deg) of $[Cu^{II}(PuPy)](ClO_4)_2$[a]

Cu(1)−N(14)	1.980(4)	N(14)−Cu(1)−N(9)	100.3(2)
Cu(1)−N(9)	1.989(4)	N(14)−Cu(1)−N(21)	82.5(2)
Cu(1)−N(21)	1.993(4)	N(9)−Cu(1)−N(21)	162.4(2)
Cu(1)−N(2)	2.008(4)	N(14)−Cu(1)−N(2)	154.9(2)
		N(9)−Cu(1)−N(2)	82.1(2)
		N(21)−Cu(1)−N(2)	102.7(2)
		θ[b]	33.0

[a] Estimated standard deviations in the least significant figure are given in parentheses. [b] Dihedral angle between planes Cu(1)−N(2)−N(9) and Cu(1)−N(14)−N(2).

Results and Discussion

X-ray Crystal Structure Analysis of $[Cu^{II}(PuPy)](ClO_4)_2$. The crystal consists of isolated $Cu^{II}(PuPy)^{2+}$ units, a perspective view of which is shown in Figure 1. Selected bond lengths and angles are listed in Table 3. The geometry of the CuN_4 coordination core is square-planar but tetrahedrally distorted. The dihedral angle θ between the plane Cu(1)−N(2)−N(9) and the plane Cu(1)−N(14)−N(21) is 33°. The Cu−N distances lie in the range 1.980−2.008 Å. The structure is disordered in the diamine bridge at carbon atom C(11). The two perchlorate anions are positioned axially to the copper with a Cu−O distance

(18) Bernasconi, C. F. *Relaxation Kinetics*; Academic Press: New York, 1976; pp 14−15.
(19) Schmid, R.; Sapunov, V. N. *Monographs in Modern Chemistry: Non-Formal Kinetics*; Verlag Chemie: Weinheim, 1982; p 25.

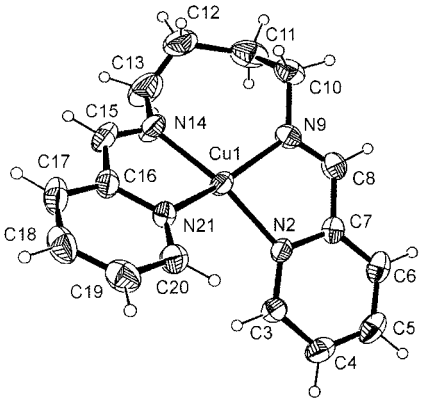

Figure 1. Molecular structure of the cation $Cu^{II}(PuPy)^{2+}$.

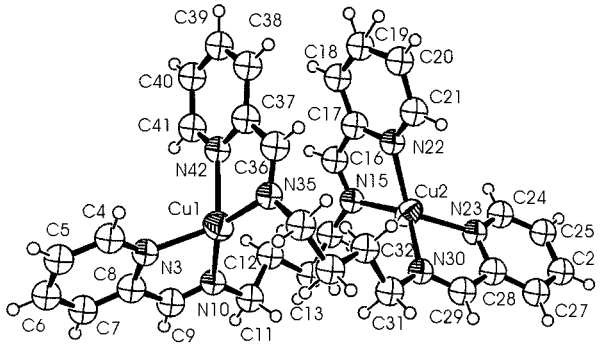

Figure 2. Molecular structure of the cation $[Cu^{I}(PuPy)]_2^{2+}$.

of 2.7 and 2.9 Å, which points to a weak interaction only. The ligand perchlorate is obviously too weak to stabilize coordination number 5, as found for the cations $Cu^{II}(PuPy)TU^{2+}$,[6] $Cu^{II}(PuPy)I^{+}$,[7] and $Cu^{II}(PuPy)Br^{+}$.[8] However, it follows from the spectrophotometric titration with pyridine that in aqueous solution the cation $Cu^{II}(PuPy)^{2+}$ tends to form the five-coordinate species $Cu^{II}(PuPy)py^{2+}$ according to eq 4 (equilibrium constant $K_{py} = 18.5\ m^{-1}$; see Table 1). It is therefore reasonable to assume for aqueous solutions of $[Cu^{II}(PuPy)](ClO_4)_2$ that in the absence of other nuceophiles the five-coordinate aquacation $Cu^{II}(PuPy)(H_2O)^{2+}$ is formed.

X-ray Crystal Structure of the Copper(I) Complex with the Ligand PuPy. The red-brown product resulting from the reaction of $Cu^{I}(CH_3CN)_4ClO_4$ with PuPy in DMF under anaerobic conditions had the composition $Cu^{I}(PuPy)ClO_4 \cdot 0.5$ DMF. The X-ray structure analysis reveals that in the solid state two units of $Cu^{I}(PuPy)^{+}$ have combined to form the dimeric species $[Cu^{I}(PuPy)]_2^{2+}$. In this binuclear cationic complex each of the two copper atoms coordinates one pyridyl nitrogen and one imine nitrogen of each ligand (see Figure 2).

The two PuPy ligands bridge the two copper atoms in a helical fashion, thus allowing almost ideal tetrahedral N_4 coordination of each copper. The dihedral angle of Cu(1) and Cu(2) is 89.63° and 89.77°, respectively. The Cu−Cu distance is 5.86 Å. The Cu−N distances lie in the range 1.9−2.1 Å (see Table 4). The individual $[Cu^{I}(PuPy)]_2^{2+}$ units are chiral, the crystal is racemic, which is in line with the space group $P\bar{1}$ (see Table 2). The distance Cu−O(perchlorate) is 4.219(1) Å, and the distance Cu−O(DMF) is found to be 4.754(1) Å, which excludes bonding interactions.

The structure of the dimer $[Cu^{I}(PuPy)]_2^{2+}$ corresponds to the dimeric structure found for the cation $Ag_2L_2^{2+}$ with the N_4 ligand

Table 4. Selected Bond Lengths (Å) and Angles (deg) of $[Cu^{I}(PuPy)]_2(ClO_4)_2 \cdot DMF$[a]

Cu(1)−N(35)	1.988(2)	N(35)−Cu(1)−N(10)	139.55(8)
Cu(1)−N(10)	2.002(2)	N(35)−Cu(1)−N(3)	125.17(8)
Cu(1)−N(3)	2.069(2)	N(10)−Cu(1)−N(3)	81.51(9)
Cu(1)−N(42)	2.105(2)	N(35)−Cu(1)−N(42)	80.78(8)
Cu(2)−N(15′)	1.924(6)	N(10)−Cu(1)−N(42)	120.17(9)
Cu(2)−N(30)	2.015(2)	N(3)−Cu(1)−N(42)	111.85(9)
Cu(2)−N(15)	2.032(3)	N(30)−Cu(2)−N(15)	127.91(10)
Cu(2)−N(23)	2.053(2)	N(30)−Cu(2)−N(23)	81.64(7)
Cu(2)−N(22)	2.061(3)	N(15)−Cu(2)−N(23)	125.77(9)
Cu(2)−N(22′)	2.107(6)	N(30)−Cu(2)−N(22)	124.08(10)
		N(15)−Cu(2)−N(22)	80.97(12)
		N(23)−Cu(2)−N(22)	122.65(10)
		θ (Cu 1)[b]	89.63(8)
		θ (Cu 2)[c]	89.77(9)

[a] Estimated standard deviations in the least significant figure are given in parentheses. [b] Angle between planes Cu(1)−N(2)−N(9) and Cu(1)−N(14)−N(21). [c] Angle between planes Cu(2)−N(15)−N(22) and Cu(2)−N(23)−N(30).

L = *N*,*N*′-bis(2-pyridyl)methylene-(*R*,*S*)-1,2-diaminocyclohexane.[20,21] The copper(I) complex with this ligand is also suggested to be dimeric.[20] Recently, Weser and co-workers[22] reported that the related N_4 ligand Pu-6-MePy (see Chart 1), carrying methyl groups in the 6-position of the pyridyl rings, forms a monomeric copper(II) complex and a dimeric copper(I) complex $[Cu^{I}(Pu\text{-}6\text{-}MePy)]_2^{2+}$ with a helical structure very similar to the one described above for the dimer $[Cu^{I}(PuPy)]_2^{2+}$. It follows from these findings that open-chain N_4 di-Schiff-base ligands, formed from pyridine-2-carbaldehyde and more or less "long" aliphatic diamines, tend to form binuclear dimeric complexes with copper(I).

Structural Aspects of the Redox System $Cu^{II}(PuPy)^{2+}$/$[Cu^{I}(PuPy)]_2^{2+}$. In the discussion of the SOD activity of the cation $Cu^{II}(PuPy)^{2+} = Cu^{II}L^{2+}$, Linss and Weser[5a,b] assumed that the reduction of $Cu^{II}L^{2+}$ (with N_4 coordination close to planar) leads to a monomeric species $Cu^{I}L^{+}$, in which L provides a distorted tetrahedral N_4 coordination for the copper(I) by intramolecular ligand rearrangement. However, it follows from the X-ray structure analysis that, as in the case of the complex $Cu^{II}(Pu\text{-}6\text{-}MePy)^{2+}$,[22] the copper(I) complex is a dimer with a helical structure. This means that the reduction of the copper(II) species is associated with a drastic change in molecular architecture, as shown schematically in

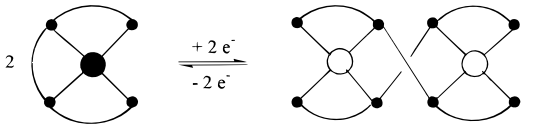

(13)

(● = Cu^{II}, ○ = Cu^{I}). The system $Cu^{II}L^{2+}/(Cu^{I}L)_2^{2+}$ can therefore be classified as a redox switch[23] that, from the structural point of view, resembles the Cu^{II}/Cu^{I} system with the N_4 ligand 5,5′,3″,5‴-tetramethyl-2,2′:6′:2″:6″:2‴-quaterpyridine described by Lehn and co-workers.[24] This ligand was the first

(20) Van Stein, G. C.; Van der Poel, H.; Van Koten, G.; Spek, A. L.; Duisenberg, J. M.; Pregosin, P. S. *J. Chem. Soc., Chem. Commun.* **1980**, 1016.
(21) Van Stein, G. C.; Van Koten, G.; Vrieze, K.; Brevard, C.; Spek, A. L. *J. Am. Chem. Soc.* **1984**, *106*, 4486.
(22) Müller, J.; Schübl, D.; Maichle-Mössmer, C.; Strähle, J.; Weser, U. *J. Inorg. Biochem.* **1999**, *75*, 63.
(23) Boulas, P. L.; Gomez-Kaifer, M.; Echegoyen, L. *Angew. Chem.* **1998**, *110*, 226.
(24) Gisselbrecht, J.-P.; Gross, M.; Lehn, J.-M.; Sauvage, J.-P.; Ziessel, R.; Piccinni-Leopardi, C.; Arrieta, J. M.; Germain, G.; Van Meersche, M. *Nouv. J. Chim.* **1984**, *8*, 661.

Table 5. Visible Absorption of the Complexes and Equilibrium Constant K_{dim} Describing the Dissociation of the Copper(I) Dimer $[Cu^{I}(PuPy)]_2^{2+}$ According to Eq 6 at 298 K

complex	λ_{max}, nm	ϵ_{max}, M^{-1} cm^{-1}	K_{dim}, M	solvent
$Cu^{II}(PuPy)^{2+}$	710	110 ± 30		water
$Cu^{II}(PuMePy)^{2+}$	711	130 ± 20		water
$Cu^{II}(PuPhPy)^{2+}$	710	120 ± 20		water
$[Cu^{I}(PuPy)]_2^{2+}$	478	13600 ± 400	*b*	water
copper(I)/PuMePy[a]	478	12000 ± 300	*b*	water
copper(I)/PuPhPy[a]	477	15900 ± 400	*b*	water
$[Cu^{I}(PuPy)]_2^{2+}$	480	13300 ± 500[c]	$(1.0 \pm 0.3) \times 10^{-4}$ [c]	acetonitrile
$[Cu^{I}(PuPy)]_2^{2+}$	480	17600 ± 400[c]	$(8 \pm 2) \times 10^{-4}$ [c]	DMF
$Cu^{I}(PuPy)S_x^{+}$	422	2600 ± 200[c]		acetonitrile
	596	1600 ± 150[c]		
$Cu^{I}(PuPy)S_x^{+}$	415	3700 ± 200[c]		DMF
	598	2400 ± 150[c]		

[a] Solution of $Cu^{II}(PuMePy)^{2+}$ and $Cu^{II}(PuPhPy)^{2+}$, respectively, after reduction with amalgenated zinc. [b] Not observed; in water the dissociation of the dimer was too small to give sufficiently large changes in absorption upon dilution. [c] Obtained by fitting eq 7 to the spectrophotometric data.

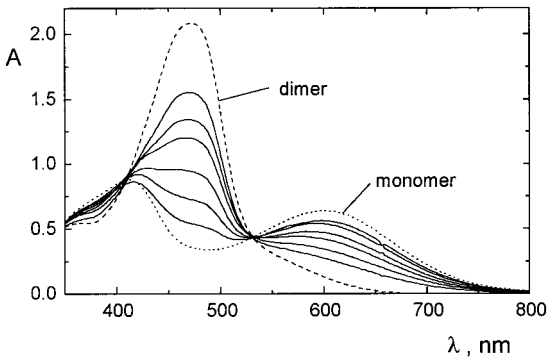

Figure 3. Spectral changes associated with the stepwise dilution of a solution of $[Cu^{I}(PuPy)]_2(ClO_4)_2$·DMF in DMF at variable path length d (0.1−5.0 cm) and $[dimer]_0 d$ = constant = 1.25×10^{-4} M (dimer, - - -; monomer, ···).

example demonstrating that upon reduction of the monomeric copper(II) complex a dimeric copper(I) helicate is formed and vice versa.

Characteristics of the Dimer/Monomer Equilibrium of the Complex $[Cu^{I}(PuPy)]_2(ClO_4)_2$ in Solution. In aqueous solution, the visible spectrum of the dimeric cation $[Cu^{I}(PuPy)]_2^{2+}$ is independent of concentration in the range $(0.025-1.25) \times 10^{-3}$ M with a maximum of absorption at λ = 478 nm (see Table 5). It is important to note that, except for small differences in ϵ_{max}, the spectra obtained for the copper(I) complexes with the substituted ligands PuMePy and PuPhPy are practically identical with the spectrum obtained for the solution of the binuclear complex $[Cu^{I}(PuPy)]_2(ClO_4)_2$ and with the spectrum of the cation $[Cu^{I}(Pu\text{-}6\text{-}MePy)]_2^{2+}$.[22] This finding strongly suggests that, in analogy to the dimeric cation $[Cu^{I}(PuPy)]_2^{2+}$, the copper(I) complexes of PuMePy and PuPhPy are also binuclear dimeric species according to $[Cu^{I}(PuMePy)]_2^{2+}$ and $[Cu^{I}(PuPhPy)]_2^{2+}$, respectively.

In the coordination of organic solvents, dissociation of the dimer $[Cu^{I}(PuPy)]_2^{2+}$ according to eq 6 occurs, as indicated by a change in absorption upon dilution. As an example, Figure 3 shows the UV/vis absorption spectra of a solution of $[Cu^{I}(PuPy)]_2(ClO_4)_2$·DMF in DMF at different concentrations with the condition $[dimer]_0 d$ = constant = 1.25×10^{-4} M being fulfilled (d = path length of the cell). Fitting of eq 7 to the data leads to the spectrum of the dimer and monomer and to the equilibrium constant K_{dim}. Table 5 summarizes the data obtained for λ_{max}, ϵ_{max}, and K_{dim} for the solvents water, acetonitrile, and DMF. It follows from these data that (i) λ_{max} and ϵ_{max} of the dimer $[Cu^{I}(PuPy)]_2^{2+}$ are practically the same for the solvents water, acetonitrile, and DMF, with ϵ_{max} for DMF being slightly higher, and that (ii) in both acetonitrile and DMF, the spectrum of the monomer is characterized by two absorption maxima at approximately 420 and 600 nm, with ϵ_{max} values of about 3000 and 2000 M^{-1} cm^{-1}, respectively. The data for ϵ_{max} are higher for DMF than for acetonitrile, which suggests that the solvent has entered the inner coordination sphere according to $Cu^{I}(PuPy)S_x^{+}$. (iii) The dissociation constant K_{dim} is 1.0×10^{-4} M for acetonitrile and 8×10^{-4} M for DMF, which means that for $[dimer]_0 = 10^{-4}$ M the degree of dimer dissociation is 39% in acetonitrile and 70% in DMF.

Table 6. Rate Constants k_M and k_D and Equilibrium Constant K_{dim} for the Equilibrium $(Cu^{I}L)_2^{2+} \rightleftharpoons 2Cu^{I}L^{+}$ According to Eq 6 in Acetonitrile and DMF at I = 0.2 M ($NaClO_4$) and 298 K

solvent	k_M, s^{-1}	k_D, M^{-1} s^{-1}	$K_{dim} = k_M/k_D$, M
acetonitrile	3.1 ± 0.2[a]	$(3.2 \pm 0.4) \times 10^4$ [a]	$(1.0 \pm 0.3) \times 10^{-4}$ [b]
DMF	1.6 ± 0.6[c]	790 ± 300[c]	$(2.0 \pm 0.8) \times 10^{-3}$
	1.0 ± 0.5[a]	1240 ± 600[a]	$(0.8 \pm 0.2) \times 10^{-3}$ [b]

[a] See ref 25 for calculation. [b] Data taken from Table 5. [c] Calculated from the slope and intercept of the plot k_{obsd}^2 vs $[M]_0$ according to eq 9; see ref 25.

One has to conclude from these results that, in contrast to water, the solvents acetonitrile and DMF are able to stabilize the monomeric copper(I) species $Cu^{I}(PuPy)S_x^{+}$, thus inducing the dissociation of the dimer $[Cu^{I}(PuPy)]_2^{2+}$.

Kinetics of Dimer/Monomer Equilibration. As described in Experimental Section, the small perturbations of equilibrium 6 in c-jump stopped-flow experiments were used to determine rate constants k_M and k_D from the plot of the linear dependence of k_{obsd}^2 on $[M]_0$ according to eq 9.[25,26] The results are summarized in Table 6.

The rate of dissociation of the dimer $[Cu^{I}(PuPy)]_2^{2+}$ in acetonitrile and in DMF is not very different (see rate constant k_M). The rate of dimerization, however, is solvent-dependent. In the solvent DMF, rate constant k_D is more than 1 order of magnitude smaller than in acetonitrile, which reflects stronger

(25) The experimentally obtained (k_{obsd},$[M]_0$) data are compiled in Table S1, and a plot of k_{obsd}^2 vs $[M]_0$ is shown in Figure S1 (acetonitrile) and Figure S2 (DMF).

(26) The slope m of the linear plot of k_{obsd}^2 vs $[M]_0$ corresponds to $8k_Mk_D$, the intercept to k_M^2. For the solvent acetonitrile, the intercept was practically zero (see Figure S1) and only $m = 8k_Mk_D$ was obtained. In this case, k_M and k_D were calulated from the slope m and the known value of K_{dim}, as obtained spectrophotometrically (see Table 5). For the solvent DMF, both slope m and intercept were obtained experimentally, which allowed us to determine k_M and k_D directly from relaxation kinetics. As shown in Figure S2, at small concentrations of M there are deviations from linearity, which are most probably due to partial oxidation of copper(I) by traces of dioxygen. These deviations were neglected in the determination of m.

Table 7. Summary of Rate Constants for Electron Transfer in the Systems $(Cu^{I}L)_2^{2+}$/Oxidant and $Cu^{II}L^{2+}$/Reductant (298 K; $I = 0.2$ M $NaNO_3$)

oxidant	reductant	solvent	k_{ox}, M^{-1} s^{-1} [a]	k_D, M^{-1} s^{-1}	k_M, s^{-1}	mechanism
$Co^{III}(NH_3)_5Cl^{2+}$	$(Cu^{I}L)_2^{2+}$	H_2O	440 ± 5[b]			A
cis-$Co^{III}(en)_2Cl_2^{+}$	$(Cu^{I}L)_2^{2+}$	H_2O	4025 ± 40			A
trans-$Co^{III}(en)_2Cl_2^{+}$	$(Cu^{I}L)_2^{2+}$	H_2O	5850 ± 70			A
$Co^{III}(NH_3)_5Cl^{2+}$	$(Cu^{I}L)_2^{2+}$	DMF	4650 ± 80[b]		0.23 ± 0.02[d]	B
$Cu^{II}L^{2+}$	$Ru^{II}(edta)(H_2O)^{2+}$	H_2O	*c*	4800 ± 100		C

[a] Second-order rate constant for oxidation according to eqs 14 and 15. [b] Ionic strength adjusted with $NaClO_4$. [c] Too fast to be observed under the given conditions. [d] This value is the mean of the experimental rate constant $k_{obsd,2}$, as obtained at five different concentrations of $[Co^{III}(NH_3)_5Cl^{2+}]$ (see Table S4).

Table 8. Temperature Dependence of Second-order Rate Constant k_{ox} for Reaction 14 with Co(III) = $Co^{III}(NH_3)_5Cl^{2+}$ in Water at $I = 0.2$ M ($NaClO_4$) and Activation Parameters

temp, K	k_{ox}, M^{-1} s^{-1}
278	97 ± 3
288	225 ± 4
298	440 ± 5
308	820 ± 16
$\Delta H^{\ddagger}$ kJ mol^{-1}	48 ± 5
$\Delta S^{\ddagger}$, J mol^{-1} K^{-1}	-34 ± 15

solvation of the monomer by DMF. It is satisfying to see that rate constants k_M and k_D, as determined from the slope and intercept of the plot k_{obsd}^2 vs $[M]_0$,[26] lead to $K_{dim} = k_M/k_D = (2 \pm 0.8) \times 10^{-3}$ M, which is rather close to the spectrophotometrically determined equilibrium constant $K_{dim} = (0.8 \pm 0.2) \times 10^{-3}$ M.

Kinetics of the Oxidation of the Copper(I) Dimer in Water. The oxidants $Co^{III}(NH_3)_5Cl^{2+}$ and *cis*- and *trans*-$Co^{III}(en)_2Cl_2^{+}$ were used to study the oxidation of the dimer $(Cu^{I}L)_2^{2+}$ in aqueous solution according to

$$(Cu^{I}L)_2^{2+} + 2Co(III) \xrightarrow{k_{ox}} 2Cu^{II}L^{2+} + 2Co(II) \quad (14)$$

under pseudo-first-order conditions ($[Co(III)] \gg [(Cu^{I}L)_2^{2+}]$). The observed decrease of the copper(I) species with time is exponential for both cobalt(III) complexes and follows eq 8. The experimental rate constant k_{obsd} increases linearly with [Co(III)] (see Tables S2 and S3 of Supporting Information), which means that second-order rate law

$$-d[dimer]/dt = k_{obsd}[dimer] = k_{ox}[Co(III)][dimer] \quad (15)$$

applies. Second-order rate constants k_{ox} are summarized in Table 7. The temperature dependence of rate constant k_{ox} for Co(III) = $Co^{III}(NH_3)_5Cl^{2+}$ and the resulting activation parameters are shown in Table 8.

The oxidation of the dimer $(Cu^{I}L)_2^{2+}$ requires 2 equiv of the oxidant Co(III). The first-order dependence on cobalt(III) suggests that k_{ox} describes the transfer of the first electron, with transfer of the second one being a fast consecutive process. The sequence of steps suggested in mechanism A describes sequential processes of the P* type,[27] which means that electron-transfer precedes structural changes ($\subset\supset$ = symbol characterizing the helical arrangement of the two ligands L in the dimer; Co(III) = $Co^{III}(NH_3)_5Cl^{2+}$ or *cis*- and *trans*-$Co^{III}(en)_2Cl_2^{+}$; charges omitted for clarity). The mixed valence species $LCu^{II}\subset\supset Cu^{I}L$, generated in reaction A1, breaks apart (eq A2) before the transfer of the second electron (eq A3). As an alternative to step A2, it is conceivable that the mixed valence dimer $LCu^{II}\subset\supset Cu^{I}L$ remains binuclear until the second copper(I) site is oxidized to form the binuclear copper(II) species $LCu^{II}\subset\supset Cu^{II}L$,

Mechanism A

$$LCu^{I}\subset\supset Cu^{I}L + Co(III) \underset{k_{-1}}{\overset{k_1}{\rightleftharpoons}} LCu^{II}\subset\supset Cu^{I}L + Co(II) \quad (A1)$$

$$LCu^{II}\subset\supset Cu^{I}L \underset{k_{-2}}{\overset{k_2}{\rightleftharpoons}} Cu^{II}L + Cu^{I}L \quad (A2)$$

$$Cu^{I}L + Co(III) \underset{k_{-3}}{\overset{k_3}{\rightleftharpoons}} Cu^{II}L + Co(II) \quad (A3)$$

$$LCu^{II}\subset\supset Cu^{I}L + CO(III) \underset{k'_{-2}}{\overset{k'_2}{\rightleftharpoons}} LCu^{II}\subset\supset Cu^{II}L + Co(II) \quad (A'2)$$

which dissociates according to

$$LCu^{II}\subset\supset Cu^{II}L \underset{k'_{-3}}{\overset{k'_3}{\rightleftharpoons}} 2Cu^{II}L \quad (A'3)$$

The spectral changes observed for reaction 14 did not provide any information on intermediate formation. There is no experimental basis therefore to discriminate between the pathways A1 → A2 → A3 and A1 → A′2 → A′3.

It is to be expected that reaction A1 is associated with substantial structural changes. The helical arrangement of the two ligands L in the copper(I) dimer has to be rearranged to provide tetrahedral coordination for the copper(I) and (distorted) square planar coordination for the copper(II) in the mixed valence species $LCu^{II}\subset\supset Cu^{I}L$. We assume that the experimentally obtained rate constant k_{ox} corresponds to rate constant k_1, describing the attack of the oxidant $Co^{III}(NH_3)_5Cl^{2+}$ and *cis*- or *trans*-$Co^{III}(en)_2Cl_2^{+}$, respectively, on the dimer $(Cu^{I}L)_2^{2+}$ according to eq A1. The activation barrier of $\Delta H^{\ddagger} = 48.5$ kJ mol^{-1}, as obtained for the oxidation with $Co^{III}(NH_3)_5Cl^{2+}$ (see Table 8), is in line with the assumption that the formation of the mixed valence dimer $LCu^{II}\subset\supset Cu^{I}L$ requires considerable structural changes.

The ratio of the corresponding rate constants obtained for oxidations with the stereoisomers *cis*-$Co^{III}(en)_2Cl_2^{+}$ and *trans*-$Co^{III}(en)_2Cl_2^{+}$ can provide mechanistic information.[28] Redox reactions following an inner sphere mechanism are by a factor of 20−30 faster with the trans isomer than with the cis isomer,[29,30] whereas for outer sphere reactions the factor is only 10.[31] In the present study, the ratio of rate constants obtained for reaction 14 is very small (k_{ox}(trans)/k_{ox}(cis) = 1.45; see Table 7). This finding possibly indicates that the course of reaction $LCu^{I}\subset\supset Cu^{I}L \rightarrow LCu^{II}\subset\supset Cu^{I}L$ is mainly controlled by changes

(27) Brunschwig, B. S.; Sutin, N. *J. Am. Chem. Soc.* **1989**, *111*, 7454.
(28) Parker, O. J.; Espenson, H. *J. Am. Chem. Soc.* **1969**, *91*, 1968.
(29) Benson, P.; Haim, A. *J. Am. Chem. Soc.* **1965**, *87*, 3826.
(30) Pennington, D. E.; Haim, A. *Inorg. Chem.* **1966**, *5*, 1890.
(31) Endicott, J. F.; Taube, H. *J. Am. Chem. Soc.* **1964**, *86*, 1686.

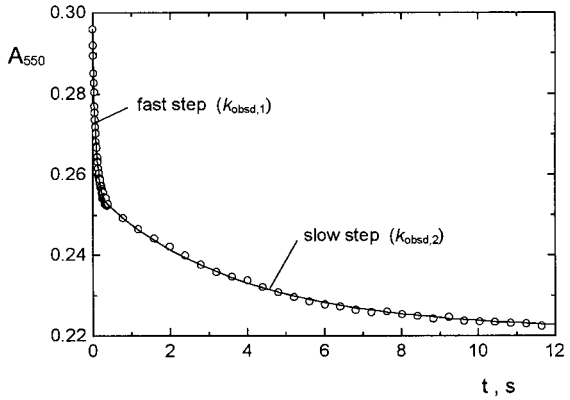

Figure 4. Time dependence of the absorbance at 550 nm for the reaction of the copper(I) dimer $Cu^{I}L_2^{2+}$ (1×10^{-4} M) with the oxidant $Co(NH_3)_5Cl^{2+}$ (2.5×10^{-3} M) in DMF at 298 K (solid line obtained by fitting of the data with eq 10).

in the arrangement of the ligands L and not affected by the stereochemistry of the oxidant $Co^{III}(en)_2Cl_2^{+}$.

Kinetics of the Oxidation of the Copper(I) Dimer with $Co^{III}(NH_3)_5Cl^{2+}$ in DMF. As pointed out above, the dimer $(Cu^{I}L)_2^{2+}$ dissociates in DMF according to equilibrium 6 with $K_{dim} = 8 \times 10^{-4}$ M. Redox reaction 14, when studied with an excess of the oxidant $Co^{III}(NH_3)_5Cl^{2+}$ in the range 300−620 nm, leads to (absorbance,time) data that can be well fitted with eq 10. This means that the overall reaction is biphasic, as shown in Figure 4 for the (A_{550},t) data. An initial fast reaction (rate constant $k_{obsd,1}$) is followed by a much slower one (rate constant $k_{obsd,2}$). Rate constant $k_{obsd,1}$ increases linearly with $[Co^{III}(NH_3)_5Cl^{2+}]$ (see Table S4), which leads to second-order rate constant $k_{ox} = 4650 \pm 80$ M^{-1} s^{-1}. Rate constant $k_{obsd,2}$ is independent of $[Co^{III}(NH_3)_5Cl^{2+}]$ (see Table S4), and the average value is found to be $k_{obsd,2} = 0.23 \pm 0.02$ s^{-1} (see Table 7). Mechanistically, it is most plausible to interpret the first step of the observed biphasic kinetics to be the second-order oxidation of the monomer $Cu^{I}L(DMF)_x^{+}$ by $Co^{III}(NH_3)_5Cl^{2+}$ (rate constants $k_{obsd,1}$ and k_{ox}, respectively). After oxidation of all of the monomer initially present at equilibrium concentration, the oxidant does not attack the dimer, as found in the solvent water. Further oxidation is instead controlled by the rate of dimer dissociation, which follows from the fact that (i) $k_{obsd,2}$ is independent of $[Co^{III}(NH_3)_5Cl^{2+}]$ and (ii) the mean value $k_{obsd,2} = 0.23 \pm 0.02$ s^{-1} is close to $k_M = 1.0 \pm 0.5$ s^{-1} and $k_M = 1.6 \pm 0.8$ s^{-1}, as determined independently from c-jump experiments (see Table 6).[32]

In contrast to the solvent water, the course of reaction 14 in the dipolar aprotic solvent DMF is basically different, as shown schematically in mechanism B (Co(III) = $Co^{III}(NH_3)_5Cl^{2+}$; charges omitted for clarity). The oxidation occurs via the

Mechanism B

$$Cu^{I}L + Co(III) \underset{k_{-1}}{\overset{k_1}{\rightleftharpoons}} Cu^{II}L + Co(II) \qquad (B1)$$

$$LCu^{I}\supset Cu^{I}L \underset{k_D}{\overset{k_M}{\rightleftharpoons}} 2\ Cu^{I}L \qquad (B2)$$

copper(I) monomer according to eq B1 with rate constant k_1 (=k_{ox}). The dissociation of the dimer according to eq B2 with rate constant k_M (=$k_{obsd,2}$) determines the rate of dimer oxidation. This mechanism is a sequential mechanism of the R*-type,[27] which means that structural changes precede electron transfer. It follows from the size of the second-order rate constant k_{ox} that the oxidation of the monomer by $Co^{III}(NH_3)_5Cl^{2+}$ in DMF is approximately 10-fold faster than the oxidation of the dimer by $Co^{III}(NH_3)_5Cl^{2+}$ in water.

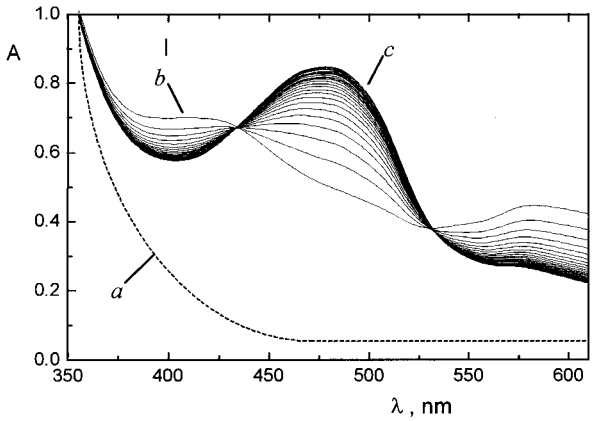

Figure 5. Spectral changes observed for the reaction of the copper(II) complex $Cu^{II}L^{2+}$ (1×10^{-4} M) with the reductant $Ru^{II}(edta)(H_2O)^{2-}$ (2×10^{-3} M) according to eq 16 in aqueous solution at 298 K (pH 6.0; $I = 0.2$ M $NaNO_3$): (a) as obtained before the reaction; (b) first spectrum obtained several milliseconds after mixing of the partners in the stopped-flow apparatus; (c) as obtained after 25 s at the end of the reaction.

Kinetics of the Reduction of the Copper(II) Complex $Cu^{II}L^{2+}$ in Water. The ruthenium(II) complex $Ru^{II}(edta)(H_2O)^{2-}$ was used to study the reduction of the copper(II) species $Cu^{II}L^{2+}$ according to

$$Cu^{II}L^{2+} + Ru(II) \xrightarrow{k_{red}} Cu^{I}L^{+} + Ru(III) \qquad (16)$$

under pseudo-first-order conditions ($[Ru(II)] \gg [Cu^{II}L^{2+}]$). The spectral changes associated with this reaction are shown in Figure 5. Spectrum a, as recorded before the reaction, changes rapidly to spectrum b. This change is too fast to be resolved on the stopped-flow time scale. Spectrum b shows the characteristic absorption pattern of the copper(I) monomer $Cu^{I}L(H_2O)_x^{+}$, whereas spectrum c corresponds to the dimer $(Cu^{I}L)_2^{2+}$. This means that according to mechanism C, there is fast initial

Mechanism C

$$Cu^{II}L + Ru(II) \underset{k_{-1}}{\overset{k_1}{\rightleftharpoons}} Cu^{I}L + Ru(III) \qquad (C1)$$

$$2\ Cu^{I}L \underset{k_M}{\overset{k_D}{\rightleftharpoons}} LCu^{I}\supset Cu^{I}L \qquad (C2)$$

electron transfer (eq C1) followed by slow dimerization (eq C2). The fact that the electron-transfer reaction (C1) is too fast to be traceable by conventional stopped-flow techniques means that the condition k_1 (=k_{red}) > 10^5 M^{-1} s^{-1} is fulfilled.

The (absorbance,time) data obtained for reaction 16, when fitted with eq 11, yield the first-order rate constant k_{obsd}. As to be expected, the size of k_{obsd} does not depend on $[Ru^{II}(edta)(H_2O)^{2-}]$ (see Table S5). Equation 12 is used to calculate first-order rate constant $k_D = 4800 \pm 100$ s^{-1} for the dimerization of the monomeric copper(I) species $Cu^{I}L(H_2O)_x^{+}$ in water. It follows from the data obtained for k_D (see Table 7) that, compared to dimerization in the solvent water, dimerization is faster in acetonitrile and slower in DMF.

(32) The data for k_M and k_D are based on a plot of k_{obsd}^2 vs $[M]_0$. As shown in Figure S2, at small concentrations of M there are deviations from linearity, which are most probably due to partial oxidation of copper(I) by traces of dioxygen. These deviations were neglected in the determination of the slope m. As a consequence of this procedure, rather high limits of error have to be assigned to the data for k_M, k_D, and K_{dim} (see Table 6).

Concluding Remarks

The compound $[Cu^{II}(PuPy)](ClO_4)_2$, introduced in 1986 by Weser and co-workers as a model complex mimicking the redox function of CuZnSOD, is a copper(II) complex with a (tetrahedrally distorted) square-planar N_4 coordination geometry. In contrast to earlier assumptions, the corresponding copper(I) complex is not monomeric. Two monomeric units of Cu^IL^+ combine to form the dimeric species $(Cu^IL)_2^{2+}$ (L = PuPy). In this binuclear complex the two ligands L bridge the two copper atoms in a helical fashion, thus allowing almost ideal tetrahedral N_4 coordination of each copper(I).

The dimer/monomer equilibrium, $D \rightleftharpoons 2M$, is solvent-dependent. In water, there is practically no dissociation of the dimer, whereas in acetontrile and DMF dissociation is substantial. The kinetics of the electron-transfer reactions $Cu^{II}L^{2+} + e^- \rightarrow Cu^IL^+$ and $(Cu^IL)_2^{2+} \rightarrow 2\ Cu^{II}L^{2+} + 2\ e^-$ are significantly affected by the kinetics of the dimerization of the monomer and dissociation of the dimer, respectively. In other words, the changes in ligand coordination associated with electron transfer in the system Cu^{II}/Cu^I/PuPy act as a redox switch. In water, cobalt(III) oxidants such as $Co^{III}(NH_3)_5Cl^{2+}$ attack the dimer $(Cu^IL)_2^{2+}$ and transfer of the first electron is rate-controlling for the overall reaction. In DMF, however, the oxidant attacks the monomer Cu^IL^+ and the dissociation of the dimer becomes rate-controlling. The reduction of $Cu^{II}L^{2+}$ by $Ru^{II}(edta)H_2O^{2-}$ is found to be too fast to be resolved by stopped-flow spectrophotometry. Experimental evidence for the intermediate formation of the binuclear mixed valence species $(LCu^ICu^{II}L)^{3+}$, presumably formed as the primary species upon oxidation of the dimer $(Cu^IL)_2^{2+}$, is not obtained under the conditions of the present study.

For the phenyl-substituted complex $Cu^{II}(PuPhPy)^{2+}$, the most effective CuZnSOD mimic so far, the spectroscopic data obtained suggest that in the copper(I) state, this complex is also dimeric.

Acknowledgment. Sponsorship of this work by the Deutsche Forschungsgemeinschaft and Verband der Chemischen Industrie e.V. is gratefully acknowledged.

Supporting Information Available: Figure S1, Figure S2, and Tables S1−S5 presenting kinetic data, Tables S6−S13 listing atomic coordinates, bond lengths and angles, anisotropic thermal parameters, and hydrogen atom coordinates for $[Cu^{II}(PuPy)](ClO_4)_2$ and $[Cu^I(PuPy)]_2(ClO_4)_2 \cdot$DMF. This material is available free of charge via the Internet at http://pubs.acs.org.

IC000097Q